Experimental Study on the Vortex Flow in a Concentric Annulus with a Rotating Inner Cylinder

Young-Ju Kim and Young-Kyu Hwang*
School of Mechanical Engineering, Sungkyunkwan University,
300 Chunchun-dong, Jangan-gu, Suwon 440-746, South Korea

This experimental study concerns the characteristics of vortex flow in a concentric annulus with a diameter ratio of 0.52, whose outer cylinder is stationary and inner one is rotating. Pressure losses and skin friction coefficients have been measured for fully developed flows of water and of 0.4% aqueous solution of sodium carboxymethyl cellulose (CMC), respectively, when the inner cylinder rotates at the speed of 0~600 rpm. Also, the visualization of vortex flows has been performed to observe the unstable waves. The results of present study reveal the relation of the bulk flow Reynolds number Re and Rossby number Ro with respect to the skin friction coefficients. In somehow, they show the existence of flow instability mechanism. The effect of rotation on the skin friction coefficient is significantly dependent on the flow regime. The change of skin friction coefficient corresponding to the variation of rotating speed is large for the laminar flow regime, whereas it becomes smaller as Re increases for the transitional flow regime and, then, it gradually approach to zero for the turbulent flow regime. Consequently, the critical (bulk flow) Reynolds number Re_c decreases as the rotational speed increases. Thus, the rotation of the inner cylinder promotes the onset of transition due to the excitation of Taylor vortices.

Key Words: Transitional Flow, Concentric Annulus, Helical Flow, Rotating Flow, Pressure Loss

Nomenclature

C_f : Skin friction coefficient
$C_{f,R}$: Skin friction coefficient with rotation
$C_{f,s}$: Skin friction coefficient without rotation
C_f^* : Relative skin friction coefficient (see Eq. (6))
D_h : Hydraulic diameter, $2(R_2-R_1)$
dp/dz : Pressure loss (Pa/m)
e : Eccentricity (mm)
m : Ratio of the eccentricity to the difference of radius
N : Rotational speed (rpm)
ΔP : Difference of pressure (Pa)
R_1 : Radius of inner cylinder (mm)
R_2 : Radius of outer cylinder (mm)
Re : Bulk flow Reynolds number, $\bar{v}_z D_h/\nu$
Re_c : Critical Reynolds number
$Re_{l,t}$: Reynolds number discriminating laminar-Taylor vortex regime and pure laminar regime
Re_ω : Rotational Reynolds number, $\omega R_1(R_2-R_1)/\nu$
Ro : Rossby number, $2\bar{v}_z/\omega R_1$
v_z : Velocity in the z-direction (m/s)
Δz : Distance between pressure taps (mm)

Greek Symbols

η : Ratio of radius, R_1/R_2
λ : Wavelength (mm)
μ : Absolute viscosity ($Pa \cdot s$)
v : Kinematic viscosity (m^2/s)

* Corresponding Author,
E-mail : ykhwang@yurim.skku.ac.kr
TEL : +82-31-290-7437; **FAX** : +82-31-290-5849
School of Mechanical Engineering, Sungkyunkwan University, 300 Chunchun-dong, Jangan-gu, Suwon 440-746, South Korea. (Manuscript **Received** January 31, 2002; **Revised** November 16, 2002)

ρ : Density of fluid (kg/m^3)
ω : Angular velocity of rotating cylinder (rad/s)

1. Introduction

Rotating flows in annular passages with rotation of a inner cylinder are important, since they have many application in bearings, rotating-tube heat exchangers and, especially, drilling of oil well where mud flows between the rotational drilling string and the fixed well casing to remove cuttings and friction-generated heat. The present study covers pressure loss problem associated with flow instability of Newtonian fluid and non-Newtonian fluid in a concentric annulus, with rotation of the inner cylinder, at various Reynolds number up to that of turbulent flow.

It is well known that the stability of a viscous flow in a small annular gap between concentric cylinders with rotation of the inner one was first considered experimentally and theoretically by Taylor (1923). He also found that the flow is stable when the inner cylinder is stationary and the outer one is rotating. Conversely, if the outer cylinder is stationary, the flow becomes unstable.

Diprima (1960) and Stuart (1958) applied the non-linear theory to investigate the relation between the Taylor number and the stability. The flow is relatively stable when the outer cylinder is rotating, and, thus, the critical (bulk flow) Reynolds number Re_c is larger and the pressure loss is smaller than that with the inner cylinder rotating (Yamada, 1962; Yamada et al., 1969; Yamada & Watanabe, 1973). The critical Reynolds number Re_c decreases as both the rotational Reynolds number Re_ω and the ratio of eccentricity m increases (Nakabayashi et al., 1974; Nouri et al., 1993 and Nouri and Whitelaw 1994).

Variations in an annular gap, wellbore eccentricity and shaft rotational speed have strong effects on pressure loss of fluid flowing in the narrow annulus of a slimhole drilling (Delwiche et al., 1992). Due to these factors, accurately calculating and controlling pressures in slimhole wellbores are difficult, when the inner cylinder rotates with a proper rotational speed below 1000 rpm, for the sake of the safety of exploration. In this case, the drilling fluid flow in the small clearance of concentric annulus has the characteristics of the vortex flow in the transitional regime.

In this study, the pressure losses and the skin friction coefficients through the rotating annulus with the diameter ratio of 0.52 have been measured under the fully developed flow condition of water and of 0.4% CMC aqueous solution. The range of the rotational speeds of the inner cylinder is between 0 and 600 rpm, which is corresponds to the range of $100 \leq Re \leq 12000$. In addition, the vortex wave in accordance with the various rotational speed and Re has been visualized to observe the effects of the rotation on the flow instability. From the present result, it is find the effects of shaft rotation (Ro), flow rate (Re) and fluid rheology on the pressure loss and flow instability by experimental work. Namely, the value of Re_c is obtained according to the various Re and rotational speed through a concentric annulus. The effect of rotation on the skin friction coefficient is significantly dependent on the flow regime. For laminar flow regime, the change of skin friction coefficient corresponding to the variation of rotating speed is large, whereas it becomes smaller as the bulk flow Reynolds number Re increases for the transitional flow regime. For turbulent flow regime, it gradually approaches to zero.

2. Data Reduction

The equation of the average axial velocity in a concentric annulus without the rotation can be expressed in terms of the pressure loss dp/dz as follows (Bird et al., 1960):

$$\bar{v}_z = \left(\frac{dp}{dz}\right)\frac{R_2^2}{8\mu}\cdot\left(\frac{1-\eta^4}{1-\eta^2} - \frac{1-\eta^2}{\ln(1/\eta)}\right) \tag{1}$$

where $\eta (= R_1/R_2)$ is the ratio of a radius. Also, the skin friction coefficient C_f can be obtained as Eq. (2),

$$C_f = \frac{dp}{dz}\cdot\frac{D_h}{2\rho\bar{v}_z^2} \tag{2}$$

where $D_h (= 2(R_2 - R_1))$ is the hydraulic diame-

ter. Equations (1) and (2) are combined as Eq. (3),

$$C_f=\frac{16}{Re}\left(\frac{1-\eta^4}{1-\eta^2}-\frac{1-\eta^2}{\ln(1/\eta)}\right)(1-\eta)^2 \qquad (3)$$

where $Re(=\rho\bar{v}_z D_h/\mu)$ is the Reynolds number. Equations (2) and (3) are used the following constants: $D_h=18.4\times10^{-3}$ m, $R_1=10\times10^{-3}$ m, $R_2=19.2\times10^{-3}$ m and $\eta=0.52$. For a concentric annulus, C_f is given as

$$C_f=\frac{23.8}{Re} \qquad (4)$$

In the experiment, the pressure losses have been measured by Eq. (5)

$$\frac{dp}{dz}=\frac{gh\sin\theta(\rho_{ccl_4}-\rho)}{\Delta z} \qquad (5)$$

where ρ, ρ_{ccl_4}, θ, h and Δz denote the density of the fluid, the density of CCl_4, the inclined angle of the manometer, the difference of head of the manometer, and the distance between pressure holes, respectively. The experimental values of the skin friction coefficients in the laminar region can be evaluated by substituting Eq. (5) into Eq. (2).

3. Experimental Apparatus, Methods and Processes

3.1 Experimental apparatus

The experimental equipments consist of a cylinder part, supporting part, fluid-providing and rotating part and measuring part which measures the flow rate, pressure loss and the temperature as shown in Fig. 1. A centrifugal pump delivered the working fluid from a supply tank to a surge tank. The fluid flowed into the annular passage with an outer brass pipe of nominal inside diameter, D_2, of 38.4 mm and 3.82 m long and an inner stainless steel rod of diameter, D_1, of 20 mm. To insure fully developed flow in the measuring section, the length of the straight pipe downstream of the test section was 2.32 m, corresponding to 126 hydraulic diameters, with a uniform step at the inlet in order to produce an artificially thickened boundary layer. The rotating cylinder with the length of 1.5 m and the non-rotating counter part are connected by bronze bearings. In order to prevent vibration and eccentricity caused by the rotation of the cylinder the connectors have been installed at three parts of the outer cylinder.

Static pressures were measured with holes of 0.5 mm diameter distributed longitudinally in the outer cylinder. The static pressures were read from a calibrated manometer bank with ±1 mm resolution. The specific gravity of the manometer fluid CCl_4 was 1.88 giving a height range of 20-600 mm. The effective viscosities used in the calculation of effective Reynolds number were obtained by determining the average wall shear stress from pressure measurements and the dividing by the shear rate determined from the power law relationship for 0.4% CMC solutions. Therefore, the effective viscosity of 0.4% CMC solution for the same flow rate of 6 LPM becomes 18 cp at 0 rpm and 22 cp at 400 rpm. The maximum uncertainties were less than ±6 and ±3% for the turbulent flow of water and of 0.4% CMC solution, respectively. The visualization device has also been installed as shown in Fig. 1. The cylinder and the rotating part have been supported by a construction H-beam of 4 m long construction steel (SK40).

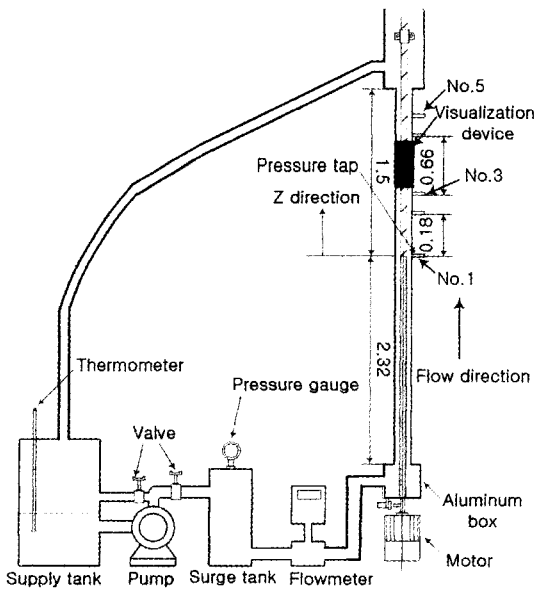

Fig. 1 Schematic diagram of experimental apparatus; all dimensions in m

The flow rate has been measured with a magnetic flow meter whose accuracy is within the limit of $\pm 0.5\%$. The temperature of the working fluid has been measured with a digital multimeter. In order to visualize a vortex flow field in a concentric annulus, a glass tube of diameter of 38.4 mm with length of 330 mm has been connected to the outer cylinder by a connector. A glass box with the thickness of 5mm filled with water has been installed to prevent diffused reflection because the visualization part is cylindrical. Particles used for visualization are PVC powders (Poly Vinyl Chloride, $\gamma=1.1$) with a mean diameter of 150 μm.

3.2 Experimental method

The development of the flow is identified by the change of the axial pressure gradient. Therefore, the value of pressure losses according to Re has been measured between the tap 1 and taps 2~5 of Fig. 1 to check the development of the flow.

In the case of water, the pressure loss along the z direction has been illustrated in Fig. 2 with various Re. Since the measured values of $\Delta P_{1,2}$ and $\Delta P_{1,3}$ have large errors due to the short distances between taps, experiments have been repeated several times to minimize the errors. The errors have appeared at the maximum of $\pm 7\%$ for ≥ 1000, because the viscosity coefficient is relatively small. The measured pressure losses along the flow of z direction at each tap are shown in Fig. 2 to confirm the development of the flow.

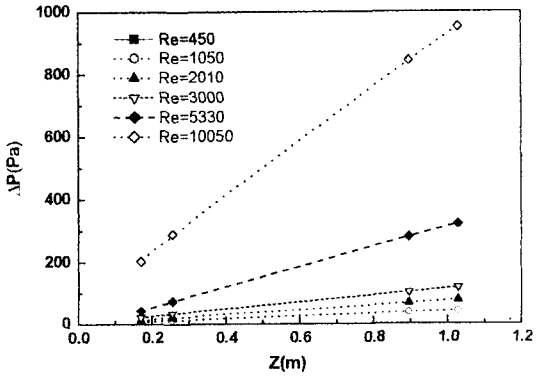

Fig. 2 Pressure differences of water as a function of z with various Re

4. Experimental Results

2.1 Pressure losses and flow characteristics

The relations between the pressure loss dp/dz and Re are shown in Fig. 3(a), for the various rotational speed in the range of water flow rate 1~60 LPM ($200 \leq Re \leq 11000$). Also, the relations between C_f and Re are shown in Fig. 3(b).

In the case of water, it is hard to measure the pressure loss accurately because it is so small for the low Re. However, in the case of 0.4% CMC solution, it is relatively easy to measure the pressure loss since its viscosity is 8 times larger than that of water. The measurement of pressure loss for 0.4% CMC solution has been carried out for $100 \leq Re \leq 12000$. Figures 4(a) and (b) show the effects of rotation on dp/dz and C_f, respectively.

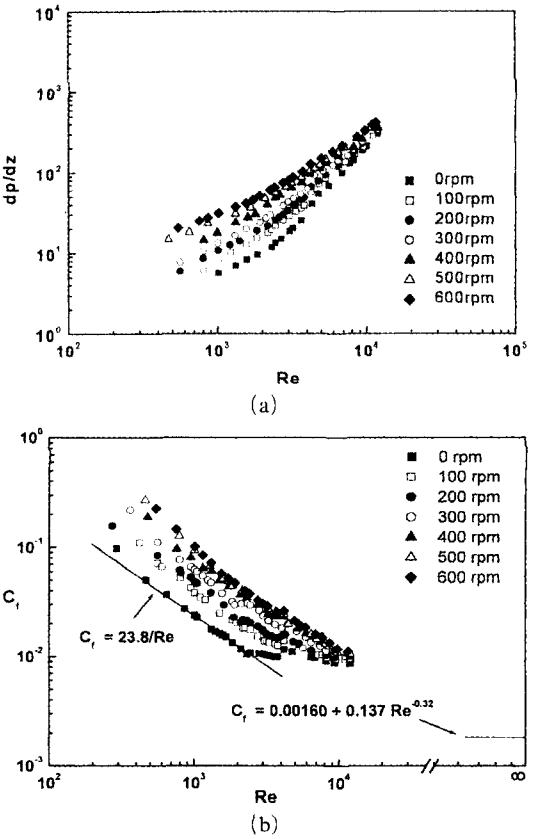

Fig. 3 (a) Pressure losses and (b) skin friction coefficients of water as a function of Re for $0 \leq N \leq 600$ rpm

The critical Reynolds number Re_c for 0.4% CMC solution has been found to be slightly lower than that for the water because of the different viscosities at the same rotational speed of as shown in Table 1.

Table 1 Variation of Re_c with respect to N and Ro

N (rpm)	Water		0.4% CMC	
	Ro	Re_c	Ro	Re_c
0	∞	2300	∞	2250
100	1.83	2170	6.70	1980
200	0.89	2100	3.16	1800
300	0.53	1900	2.04	1720
400	0.37	1736	1.47	1600
500	0.27	1597	1.13	1480
600	0.21	1500	0.89	1340

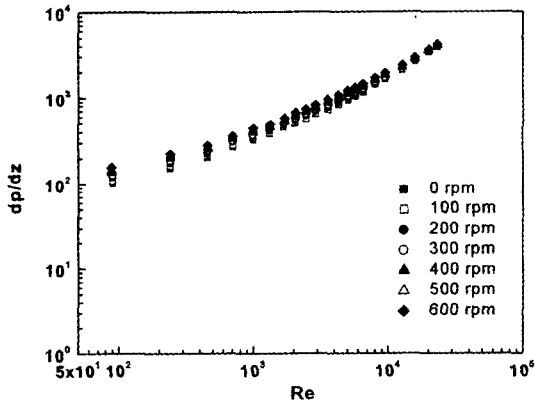

(a)

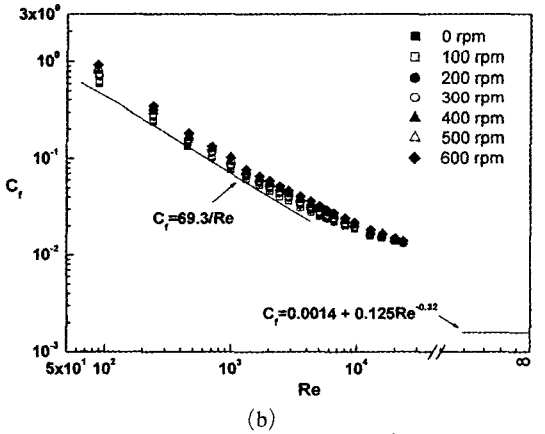

(b)

Fig. 4 (a) Pressure losses and (b) skin friction coefficients of 0.4% CMC as a function of Re for $0 \leq N \leq 600$ rpm

4.4.1 Laminar regime

Laminar regime has been confined to the range $Re < Re_c$, where, Re_c decreases according to the increase of rotational speed as shown in Table 1. From the experimental result of pressure losses for both water and 0.4% CMC solution, the gradient of the skin friction coefficients is almost irrespective of the change of rotational speed N for $N < 200$ rpm, but it becomes steeper for $N \geq 300$ rpm as N increases as shown in Figs. 3 and 4.

The relative skin friction coefficient C_f^* is defined as Eq. (6) where, suffixes s and R represents the skin friction coefficient for rotation and for non-rotation, respectively.

$$C_f^* = [(C_{f,R} - C_{f,s}) / C_{f,R}] \tag{6}$$

We can obtain C_f^*, in the case of water, by Eq. (6) as shown in Fig. 5. The value of C_f^* significantly increases from 40 to 76% in the laminar regime as N increases from 100 to 400 rpm. On the other hand, in the case of 0.4% CMC solution, the value of C_f^* slightly increases from 4 to 26% as N increases from 100 to 400 rpm. Namely, the influence of the rotational speed on the pressure losses for 0.4% CMC solution is relatively weaker than that for the water, because the value of Rossby number Ro for 0.4% CMC solution is larger than that for water (i.e., $Ro \geq 0.7$). Note that Ro is the ratio of Re_ω to Re, which represents the ratio of Coriolis to inertial forces.

The pressure losses for 0.4% CMC solution are shown in Fig. 6. The previous researchers also

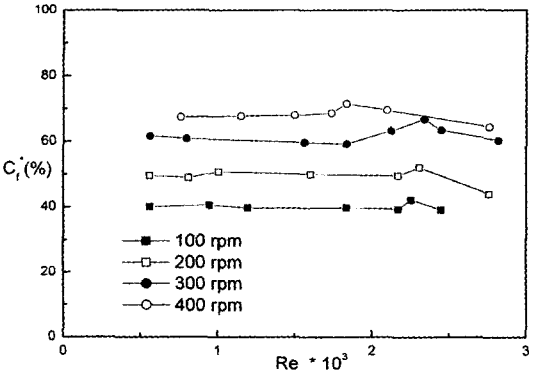

Fig. 5 Normalized relative skin friction coefficients C_f^* of water with Re at $N = 100 \sim 400$ rpm

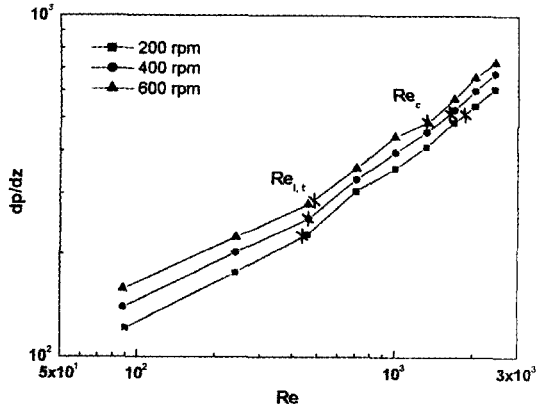

Fig. 6 Pressure losses of 0.4% CMC as a function of Re at N=200, 400 and 600 rpm

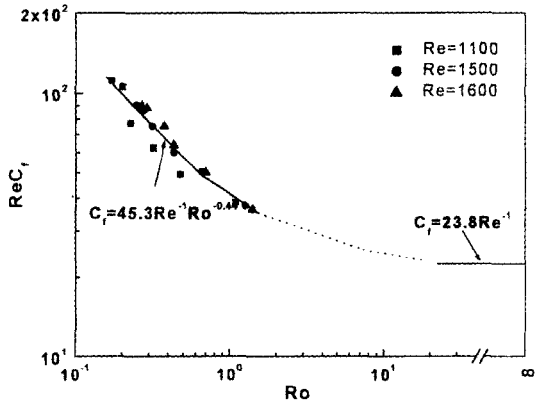

Fig. 7 Relation of C_fRe with Ro for laminar flow in water

observed that laminar-Taylor vortex exists in the range of $131 \leq Re \leq 927$ (Wereley and Lueptow, 1994).

It is found from the present results that the laminar-Taylor vortex exists in the range $0 \leq Re \leq Re_{l,t}$. The value of $Re_{l,t}$ increases as N increases and, at the same time, Ro decreases (see Table 1). If the bulk flow increases for $Re > Re_{l,t}$, the flow belongs to the laminar flow regime where the Taylor vortex has the least influence.

The Figs. 7 and 8 show the relation between $C_f \cdot Re$ and Ro in the case of water and 0.4% CMC solution, respectively. Thus, the skin friction coefficient C_f can be correlated with Ro and Re as Eq. (7) and for water and Eq. (8) for 0.4 % CMC solution, respectively.

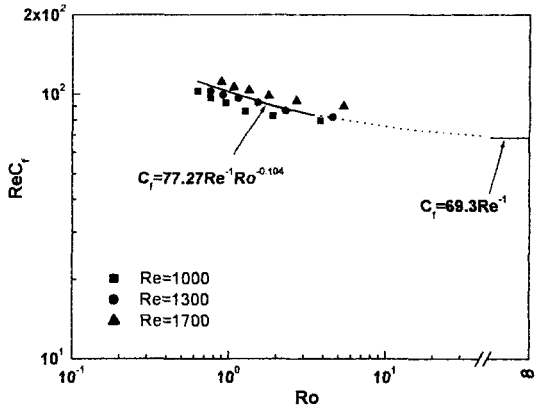

Fig. 8 Relation of C_fRe with Ro for laminar flow in 0.4% CMC

$$C_f\mathrm{Re}=45.3\ Ro^{-0.44} \tag{7}$$

$$C_f\mathrm{Re}=77.27\ Ro^{-0.104} \tag{8}$$

The deviation of experimental data with the correlations is within ±9%. As Ro becomes infinite it tends to approach to Eq. (9) for water and Eq. (10) for 0.4% CMC solution, asymptotically.

$$C_f=23.8Re^{-1} \tag{9}$$

$$C_f=69.3Re^{-1} \tag{10}$$

4.1.2 Transitional regime

From the experimental results, the critical Reynolds number Re_c is dependent on the rotational speed N and the Rossby number Ro as shown in Table 1 and Fig. 6. Although many controversies have arisen regarding the true distinction between laminar and turbulent flow of non-Newtonian fluid, the change of pressure gradient is used in this study. The value of Re_c decreases as N increases. At the same time, Re_c decreases as Ro decreases.

If C_f^* is used to express the influence of N (i.e., Re_ω) on the skin friction coefficients, C_f^* is consistently unchanged in the laminar regime as seen in Fig. 5. But, C_f^* tends to increase in the transition regime for $Re \approx Re_c$, and to decrease in the turbulent regime (i.e, $Re \gg Re_c$). However, this tendency decreases as N increases, due to the Taylor vortex. The increased rate of skin friction coefficient $C_{f,R} - C_{f,s}/C_{f,s}$ due to the rotation is about 65% in the case of water at N=100 rpm.

4.1.3 Turbulent regime

In the case of water, the skin friction coefficient C_f can be correlated with Re as Eq. (11) in Fig. 3(b) for 9000.

$$C_f=0.0016+0.137Re^{-0.32} \quad (11)$$

According to Eqs. (9) and (11), the change of C_f corresponding to variation of Re in a laminar regime is larger than that in a turbulent regime. The measured values are up to 10% smaller than those of Eq. (12) from by Nouri et al. (1993).

$$C_f=0.36Re^{-0.39} \text{ for } 4000<Re<30000 \quad (12)$$

If the material of the cylinder and the difference of the radius ($\eta=0.5$) of the concentric annulus are considered, in the case of 0.4% CMC solution, the measured values are up to 5% smaller than those of Eq. (13) from Metzner and Reed(1955).

$$C_f=0.0014+0.125Re^{-0.32} \quad (13)$$

4.2 Flow visualization

In the case of water, Taylor vortices were observed between the rest outer cylinder and the inner cylinder rotating. Photos 1 and 2 show Taylor vortices for $Re=0$ at $N=100$ and 150 rpm, respectively. When the flow rate was zero, the Taylor vortex could not be observed for $N<$ 50 rpm, due to the small effect of rotation on the flow. The wavelength λ is defined as the length of a pair of the Taylor vortex. The value of λ is 20 mm at $N=100$ rpm (see Photo 1). For $200<N<300$ rpm at $Re=0$, the wavelength was not observed clearly because increase of rotational speed is promoted in the turbulent effect. After the Taylor vortices break down, the rotating flow between the coaxial cylinders becomes turbulent flow. Thus, the Taylor vortex could not be observed for $N>400$ rpm due to the turbulent effect. This physical phenomenon is very important for considering the rotating flow between the coaxial cylinders. When the gap between the outer rest cylinder and the inner rotating cylinder becomes wide, the wavelength of the Taylor vortices becomes longer with lapse of time. If the gap between the inner and outer cylinders is very narrow, the wavelength λ of the Taylor vortices can be predicted by Eq. (14) from Ogawa (1993).

$$\lambda=R_1(116.8/Re_\omega)^{2/3}(\text{mm}) \quad (14)$$

As the rotational speed N is changed from 100 to 150 rpm, the theoretical value of λ obtained

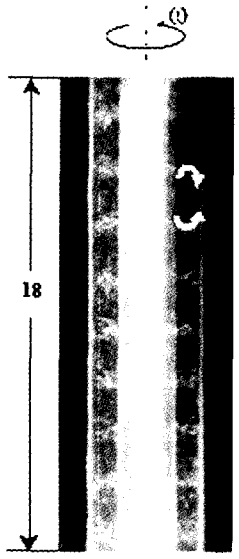

Photo 1 Taylor vortices with rotation of inner cylinder at 100 rpm ($Re=0$)

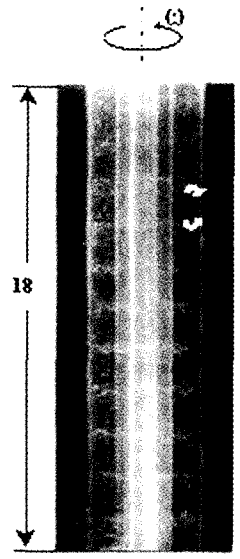

Photo 2 Taylor vortices with rotation of inner cylinder at 150 rpm ($Re=0$)

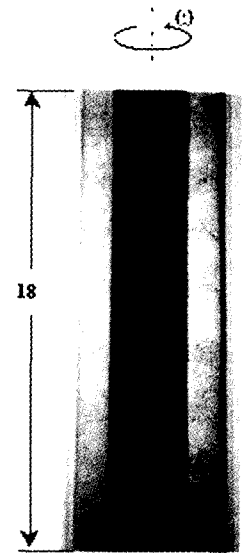

Photo 3 Taylor vortices with rotation of inner cylinder at 100 rpm ($Re=400$)

by Eq. (14) is decreased by 23%, but the measured λ from Photo 1 is decreased by 17.3% approximately. Because the above Eq. (14) is only available in the case of narrow gap $\eta > 0.8$, the theoretical λ is different with the experimental λ in the case of $\eta = 0.52$. The wavelength is significantly influenced by the rotation and the size of gap between the concentric cylinders.

Even though the wavelength was not observed for $Re = 500$ at $N = 80$ rpm, the existence of the spiral flow was observed. The spiral flows with Taylor vortices were observed for $Re = 400$ at $N \geq 100$ rpm, since the effect of rotation on the flow is large. When Re is in the range of $500 \leq Re \leq 1300$, the observed waves show unstable behavior. For example, photo 3 in the case of $Re = 400$ at $N = 100$ rpm, shows the wavelength of 28 mm which is longer than that in the case without the bulk flow.

If the bulk flow exists, it is difficult to compare its wavelength because of deficient data of the wavelength according to the change of the rotational speed. However, it is found that the wavelength decreases as the rotational speed increases, which was also observed by Becker and Kaye (1962).

5. Conclusions

In this study, the effects of the rotational speeds, the flow rates and the working fluids on the pressure losses and skin friction coefficients have been investigated experimentally for the rotating flow between the rest outer cylinder and the inner cylinder rotating. From the present results, the new correlations among the skin friction coefficients, the Rossby numbers, and Reynolds numbers have been presented within the reasonable limits of the accuracy in the laminar regimes.

It is clear that the critical Reynolds number Re_c of 0.4% CMC has a slightly lower value than that of water due to the difference of rheological characteristics. The pressure loss slightly increases as the rotational speed increases although the relative skin friction coefficient C_f^* decreases as the bulk Reynolds number Re increases in the regimes of the transition and turbulence. The value of Re_c decreases if the rotational speed increase (i.e., Rossby number Ro decreases). Also, the strong flow disturbances caused by the Taylor vortex between the concentric cylinders results in decrease of Re_c and, also, the increase of C_f. The effect of the rotation on the pressure loss is significantly smaller in the turbulent regime than that in the laminar regime.

The Rossby number of the water is smaller than that of 0.4% CMC solution. Thus, the effects of rotation on the pressure loss in water are much greater than that in 0.4% CMC solution.

The distinct Taylor vortex has been observed at 50~130 rpm for the zero bulk flow rate. When the bulk flow exists, the Taylor vortex has been observed at the rotational speed of 100 rpm for $Re = 400$. Also, it is shown that the Taylor vortex has a significant effect on the flow transition for small Re, since the wavelength decreases as the rotational speed increases.

Acknowledgment

This work was supported by the academy research fund of the Korea Energy Management Corporation.

References

Becker, K. M. and Kaye, J., 1962, "Measurements of Adiabatic Flow in an Annulus With an Inner Rotating Cylinder," *J. Heat Transfer*, Vol. 84, pp. 97~105.

Bird, R. B., Lightfoot, E. N. and Stewart, W. E., 1960, *Transport Phenomena*, pp. 34~70.

Delwiche, R. A., Lejeune, M. W. D. and Stratabit, D. B., 1992, "Slimhole Drilling Hydraulics," *Society of Petroleum Engineers Inc.*, SPE 24596, pp. 521~541.

Diprima, R. C., 1960, "The Stability of a Viscous Fluid Between Rotating Cylinders with an Bulk Flow," *J. Fluid Mech.*, Vol. 366, pp. 621~631.

Maeda, K., Nakabayashi, K. and Yamada, Y., 1969, "Pressure Drop of the Flow through Eccentric Cylinder with Rotating Inner Cylinders," *Bull. JSME*, Vol. 12, No. 53, pp. 1032~1040.

Metzner, A. B. and Reed, J. C., 1955, "Flow of

Non-Newtonian Fluids-Correlation of the Laminar, Transition, and Turbulent-flow Regions," *AIChE Journal*, Vol. 1 No. 4, pp. 434~440.

Nakabayashi, K., Seo, K. and Yamada, Y., 1974, "Rotational and Axial through the Gap between Eccentric Cylinders of which the Outer One Rotates," *Bull. JSME*, Vol. 17, No. 114, pp. 1564~1571.

Nouri, J. M., Umur, H. and Whitelaw, J. H., 1993, "Flow of Newtonian and Non-Newtonian Fluids in Concentric and Eccentric Annuli," *J. Fluid Mech.*, Vol. 253, pp. 617~641.

Nouri, J. M. and Whitelaw, J. H., 1994, "Flow of Newtonian and Non-Newtonian Fluids in a Concentric Annulus With Rotation of the Inner Cylinder," *J. Fluids Eng.*, Vol. 116, pp. 821~827.

Ogawa, A., 1993, *Vortex Flow*, CRC Press Inc., pp. 169~192.

Stuart, J. T., 1958, "On the Nonlinear Mechanics of Hydrodynamic Stability," *J. Fluid Mech.*, Vol. 4, pp. 1~21.

Taylor, G. I., 1923, "Stability of a Viscous Fluid Contained Between Two Rotating Cylinders," *Phil. Trans. A*, Vol. 223, pp. 289~343.

Watanabe, S. and Yamada, Y., 1973, "Frictional Moment and Pressure Drop of the Flow through Co-Axial Cylinders with an Outer Rotating Cylinder," *Bull. JSME*, Vol. 16, No. 93, pp. 551~559.

Wereley, S. T. and Lueptow, R. M., 1998, "Spatio-Temporal Character of Non-Wavy and Wavy Taylor-Couette Flow," *J. Fluid Mech.*, Vol. 364, pp. 59~80.

Yamada, Y., 1962, "Resistance of a Flow through an Annulus with an Inner Rotating Cylinder," *Bull. JSME*, Vol. 5, No. 18, pp. 302~310.